Acta Crystallographica Section D
Biological Crystallography
ISSN 1399-0047

Structure of *Escherichia coli* Grx2 in complex with glutathione: a dual-function hybrid of glutaredoxin and glutathione *S*-transferase

Jun Ye,[a] S. Venkadesh Nadar,[b] Jiaojiao Li[b] and Barry P. Rosen[b]

[a]Key Laboratory of Urban Environment and Health, Institute of Urban Environment, Chinese Academy of Sciences, Xiamen, People's Republic of China, and [b]Department of Cellular Biology and Pharmacology, Florida International University, Herbert Wertheim College of Medicine, Miami, FL 33199, USA

Received 28 September 2013
Accepted 24 April 2014

PDB references: Grx2–GSH complex, 4kx4; Grx2 C9S/C12S mutant, 4ksm

The structure of glutaredoxin 2 (Grx2) from *Escherichia coli* co-crystallized with glutathione (GSH) was solved at 1.60 Å resolution. The structure of a mutant with the active-site residues Cys9 and Cys12 changed to serine crystallized in the absence of glutathione was solved to 2.4 Å resolution. Grx2 has an N-terminal domain characteristic of glutaredoxins, and the overall structure is congruent with the structure of glutathione *S*-transferases (GSTs). Purified Grx2 exhibited GST activity. Grx2, which is the physiological electron donor for arsenate reduction by *E. coli* ArsC, was docked with ArsC. The docked structure could be fitted with GSH bridging the active sites of the two proteins. It is proposed that Grx2 is a novel Grx/GST hybrid that functions in two steps of the ArsC catalytic cycle: as a GST it catalyzes glutathionylation of the ArsC–As(V) intermediate and as a glutaredoxin it catalyzes deglutathionylation of the ArsC–As(III)–SG intermediate.

1. Introduction

Glutaredoxins are oxidoreductases (Fernandes & Holmgren, 2004) that belong to the thioredoxin (Trx) superfamily (Martin, 1995). They are ubiquitous in most living organisms, from bacteria to humans, and are found in some viruses. Their primary function is to maintain the reduced state of cysteine residues in intracellular proteins, and they are involved in the reduction of proteins during oxidative stress (Ströher & Millar, 2012). *Escherichia coli* Grx1 was the first identified glutaredoxin, and it functions as a GSH-dependent electron donor for ribonucleotide reductase (Holmgren, 1976). Grxs can reduce mixed disulfides between proteins and GSH, a process termed deglutathionylation. There are two mechanisms for deglutathionylation. One is a monothiol reaction in which only the N-terminal cysteine residue is required for reducing the mixed disulfide. The other is a dithiol reaction in which both active-site cysteine residues form an intramolecular disulfide bond during the reduction of protein disulfides (Stroher & Millar).

Most organisms have several glutaredoxin isoforms. *E. coli* has four, Grx1, Grx2, Grx3 and Grx4, which fall into three categories in terms of structural and catalytic properties. Grx1 and Grx3 are classical 10 kDa glutaredoxins with two conserved active-site cysteine residues in a CPYC motif that fall into the first category. Grx2 also has a CPYC motif, but is larger at 215 residues (24 532 Da) and belongs to the second category. Grx4 is in the third category with a monothiol active-site motif CGFS (Holmgren, 1976; Åslund *et al.*, 1994, 1996; Fernandes *et al.*, 2005).

Table 1
Summary of diffraction data and structure-refinement statistics.

Values in parentheses are for the highest resolution shell.

	Grx2–GSH	Grx2 C9S/C12S
Data collection		
Wavelength (Å)	1.0000	1.5418
Space group	$P3_221$	$P2_12_12_1$
Unit-cell parameters (Å)	$a = b = 50.10$, $c = 152.47$	$a = 28.16$, $b = 78.65$, $c = 89.16$
Resolution range (Å)	22.47–1.60 (1.69–1.60)	29.49–2.40 (2.49–2.40)
$R_{\rm merge}$ (%)	6.2 (10.0)	15.0 (40.7)
$\langle I/\sigma(I)\rangle$	20.6 (4.7)	5.0 (1.8)
Completeness (%)	94.8 (67.0)	98.7 (99.1)
Multiplicity	6.5 (1.5)	3.3 (3.5)
Unique reflections	28685 (2853)	8139 (785)
Refinement		
R factor/$R_{\rm free}$ (%)	16.2/19.6	20.6/28.0
No. of protein atoms	1722	1731
No. of ligand atoms	24	8
No. of water molecules	301	79
B factors (Å^2)		
Protein	11.38	40.78
Ligand	11.75	52.18
Water	22.03	43.17
R.m.s.d., bond lengths (Å)	0.006	0.007
R.m.s.d., bond angles (°)	1.24	1.17
Ramachandran plot (%)		
Outliers	0	0
Allowed	1.4	2.8
Favored	98.6	97.2
PDB code	4kx4	4ksm

Grx2 distinguishes itself from the other three glutaredoxins by its abundance in the cell (Vlamis-Gardikas *et al.*, 1997), its relatively large molecular weight, its low sequence similarity and its unique kinetic properties. Unlike the other Grxs, it is not an electron donor to ribonucleotide reductase (Vlamis-Gardikas *et al.*, 1997). Although Grx2 can reduce mixed disulfides between protein cysteine thiolates and GSH, it is not as efficient as the other glutaredoxins (Lundström-Ljung *et al.*, 1999). The only primary function identified for Grx2 is that it is the most effective hydrogen donor for reduction of arsenate by plasmid R773 ArsC arsenate reductase, and its catalytic efficiency is considerably higher than the other three *E. coli* glutaredoxins (Shi *et al.*, 1999).

The NMR structure of reduced Grx2 from *E. coli* shows that it has an N-terminal domain with a conserved Trx fold motif (Xia *et al.*, 2001) and a C-terminal domain that is not present in the other three glutaredoxins but is structurally similar to the C-terminal domain of glutathione *S*-transferases (GSTs), in particular the human ω-class GST (Board *et al.*, 2000). However, owing to the lack of structural information on the *E. coli* Grx2–GSH complex or on the oxidized form of Grx2 and its catalytic properties, the mechanism of the reduction of mixed disulfides by Grx2 remains unclear. Here, we describe the crystal structures of the glutathione-bound complex and a C9S/C12S double mutant Grx2 which mimics the reduced form. Purified Grx2 exhibited GST activity towards the artificial substrate 1-chloro-2,4-diatrobenzene (CDNB), as do authentic GSTs. Rigid-body docking of Grx2 with ArsC using the *ZDOCK* server suggests that the C-terminal domain is involved in interaction with ArsC, which has been proposed to undergo a catalytic cycle involving the formation of an ArsC–As(V)–SG intermediate and reduction to an ArsC–As(III)–SG intermediate, which is deglutathionylated with release of the product, As(III). We propose that Grx2 is a novel Grx/GST hybrid that functions as a GST in glutathionylation of the ArsC–As(V) intermediate and as a Grx in deglutathionylation of the ArsC–As(III)–SG intermediate.

2. Materials and methods

2.1. Structure determination and refinement

The crystallization and X-ray data collection of the Grx2–GSH complex and the Grx2 C9S/C12S mutant have been reported by Sheng *et al.* (2007). The Grx2–GSH complex structure was solved by molecular replacement with *AMoRe* (Navaza, 2001) using the first conformer of the NMR structure of reduced Grx2 (PDB entry 1g7o; Xia *et al.*, 2001) as an initial model. The Matthews coefficient of 2.3 Å^3 Da^{-1} suggests that one protein molecule is present in the asymmetric unit. The best solution, with an R factor of 46.3% and a correlation coefficient of 49.3%, was used for further model building. 20 cycles of rigid-body refinement and 20 cycles of restrained refinement in *REFMAC*5 (Murshudov *et al.*, 2011) improved the correlation coefficient to 76% and reduced the R factor to 37%. The side chains and GSH molecule were fitted into the electron-density map using *Coot* (Emsley *et al.*, 2010). The electron density for GSH and the Cys9 residue clearly show that there is no disulfide bond between them. Water molecules were added at various stages of refinement. One cycle of simulated-annealing refinement was carried out in *PHENIX* (Adams *et al.*, 2010). A randomly selected 5% of the reflections were used as a test set for the calculation of $R_{\rm free}$. All side chains were used in the refinement. The electron density ($2F_{\rm o} - F_{\rm c}$ map) of the backbone atoms and all side-chain atoms are complete at the 1σ contour level. The final values of the R factor and $R_{\rm free}$ were 16.4 and 19.4%, respectively. Models were generated using *Chimera* (Pettersen *et al.*, 2004). Models of electron-density maps were generated using *PyMOL* (DeLano, 2002).

The Grx2 mutant structure was also solved by molecular replacement with *AMoRe* using the partially refined Grx2–GSH structure as an initial model. There is one molecule in the asymmetric unit. The refinement was carried out as above. The final R factor and $R_{\rm free}$ values were 20.6 and 28.0%, respectively. The electron density (contoured at the 1σ level) of all backbone and side-chain atoms are complete except for the side chains of Arg57 and Lys81. The refinement statistics are summarized in Table 1. Electron-density maps of the active sites of both structures are shown in Supplementary Fig. S1[1]. Coordinates and structure factors have been deposited for the Grx2–GSH complex (PDB entry 4kx4) and the Grx2 C9S/C12S mutant (PDB entry 4ksm).

[1] Supporting information has been deposited in the IUCr electronic archive (Reference: KW5084).

2.2. GST activity

Grx2 was purified as described by Shi *et al.* (1999). *Schistosoma japonicum* GST (sjGST) was expressed from *E. coli* bearing plasmid pET-41a+ and was purified by Ni–NTA affinity chromatography using the same conditions as for Grx2. GST activity was measured using 0.3 µ*M* of either purified Grx2 or sjGST in an assay buffer consisting of 0.1 *M* potassium phosphate pH 6.5, 2.5 m*M* reduced GSH and the indicated concentrations of CDNB (Habig *et al.*, 1974; Mannervik & Danielson, 1988; Wilce & Parker, 1994). After pre-incubation at 37°C for a few minutes, Grx2 was added to initiate the reaction, which was followed by the change in absorption at 340 nm. The concentration dependence for GSH was assayed with 4 m*M* CDNB, and the concentration dependence for CDNB was assayed with 1 m*M* GSH.

2.3. Docking of ArsC–Grx2

The *E. coli* ArsC crystal structure (PDB entry 1i9d; Martin *et al.*, 2001) was used to analyze ArsC–Grx2 interactions. Two sets of coordinates without water molecules, the ArsC–Grx2–GSH full structure and ArsC–Grx2–GSH with the C-terminal domain eliminated, were submitted to the *ZDOCK* (v.ZD3.02) server (Pierce *et al.*, 2011) and the five top-ranked predictions were minimized using *NAMD*2 (Phillips *et al.*, 2005) and *VMD* (Humphrey *et al.*, 1996). GSH is a tripeptide with the γ-carboxylate of glutamic acid attached to the amino-terminus of the dipeptide Cys-Gly. The *ZDOCK* server does not accept GSH directly as a ligand, so the neutral form of the tripeptide Glu-Cys-Gly was used to approximate GSH for docking analysis. The coordinates of a minimized model (ArsC–Grx2–GSH) are available as Supporting Information.

3. Results

3.1. Overall structure

As predicted, the crystal structure of the Grx2–GSH complex shows an N-terminal domain, a C-terminal domain and one bound GSH molecule. The N-terminal domain (residues 1–72) adopts a topology similar to that of a thioredoxin fold, with four β-sheets flanked by three α-helices (Fig. 1). From the N-terminus, the structure begins with a β-strand (β1) followed by an α-helix (α1) and a second β-strand (β2) that is parallel to β1. Helix α2 connects strands β2 and β3. Strand β3 is antiparallel to strands β1 and β2. Strand β4 is antiparallel to β3, and its end leads to the third α-helix. The four β-sheets are almost in the same plane, with helices α1 and α3 below this plane and helix α2 above it and facing the solvent. The C-terminal domain consists of eight α-helices and two 3_{10}-helices. One 3_{10}-helix is between helices α4 and α5. The other 3_{10}-helix is located just before the C-terminus. Helices α4, α6 and α7 form a three-helix bundle, with helix α8 almost perpendicular to it. An 11-residue linker connects the N-terminal and C-terminal domains. The Grx2–GSH structure is similar to that of glutathione-bound Grx2 from *Salmonella typhimurium* (PDB entry 3ir4; Center for Structural Genomics of Infectious Diseases, unpublished work). The root-mean-square deviation (r.m.s.d.) of the main-chain atoms of both structures is 0.45 Å and the sequence identity is 82.6%.

3.2. Comparison of the Grx2–GSH and Grx2 C9S/C12S structures

The reduced form of Grx2 did not crystallize, but the Grx2 C9S/C12S mutant did, so this structure was used to approximate that of the reduced form. The mutant enzyme and Grx2–GSH complex were crystallized under nearly the same

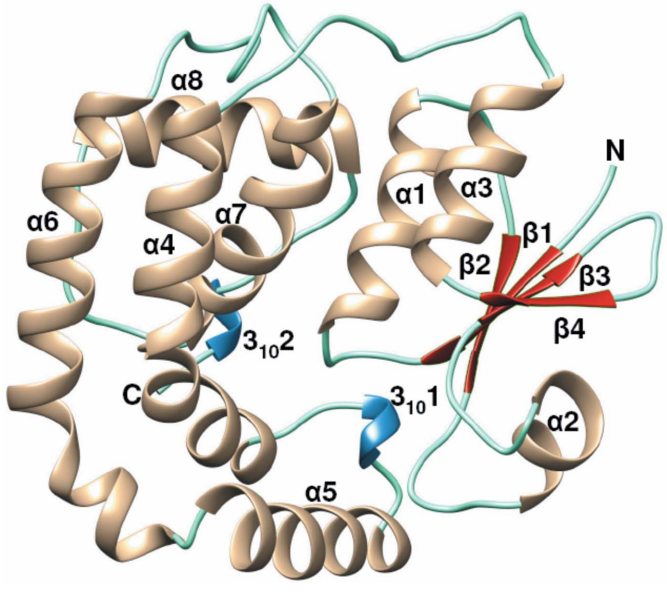

Figure 1
Ribbon diagram of the Grx2–GSH complex (PDB entry 4kx4). Secondary-structural elements: α-helix, tan; β-sheet, brown; coil, cyan; 3_{10}-helix, blue.

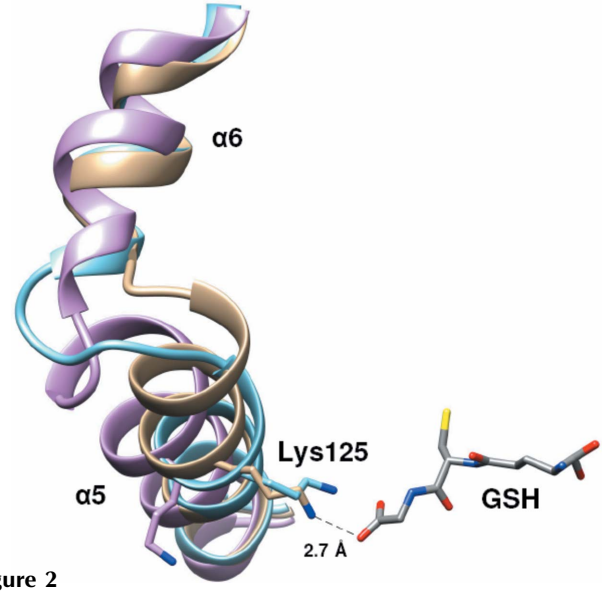

Figure 2
Superimposition of helices α5 and α6 of the Grx2–GSH complex (PDB entry 4kx4; tan) with the structure of the Grx2 C9S/C12S mutant (cyan; PDB entry 4ksm) and the NMR model (orchid; PDB entry 1g7o) of Grx2 .

conditions, so that conformational changes upon GSH binding can be best represented by comparison of the two structures. The r.m.s.d. between the main-chain atoms of the Grx2–GSH and Grx2 C9S/C12S structures is 1.13 Å. All of the residues of the mutant structure superimposed with the Grx2–GSH structure except for Ala128, Ser129, Ala130 and Gly131. If these residues are excluded, the r.m.s.d. becomes 0.57 Å, indicating that this region contributes most of the differences between the two structures. α5 extends to Ser129 in Grx2–GSH, but in the Grx2 C9S/C12S structure Ala128 and Ser129 break the hydrogen bonds necessary for forming an α-helix (Fig. 2). The electron-density maps of these regions in both structures are shown in Supplementary Fig. S2. The backbone of these residues in the Grx2–GSH structure superimposed with that of Grx2 from *S. typhimurium*, which also has GSH at its binding site. The *S. typhimurium* Grx2 backbone atoms matched well with the *E. coli* Grx2–GSH structure but not with the Grx2 C9S/C12S structure. When the 21st model of the NMR structure of reduced *E. coli* glutaredoxin (Xia *et al.*, 2001) was compared with our wild-type Grx2–GSH and Grx2 C9S/C12S crystal structures, they were nearly superimposable except for a portion of helix α5 and the linker between α5 and α6 (Fig. 2). When all 21 NMR structural models were superimposed on the Grx2–GSH and Grx2 C9S/C12S crystal structures, helix α5 and the linker exhibit the greatest mobility (Supplementary Fig. S3). In the NMR structures, the length of helix α5 is more like that of Grx2 C9S/C12S than the wild type, but its helical axis deviates from that of the crystal structures. In the wild-type Grx2–GSH structure, Lys125 makes a salt bridge to the carboxylate O atom of the glycyl residue of GSH,

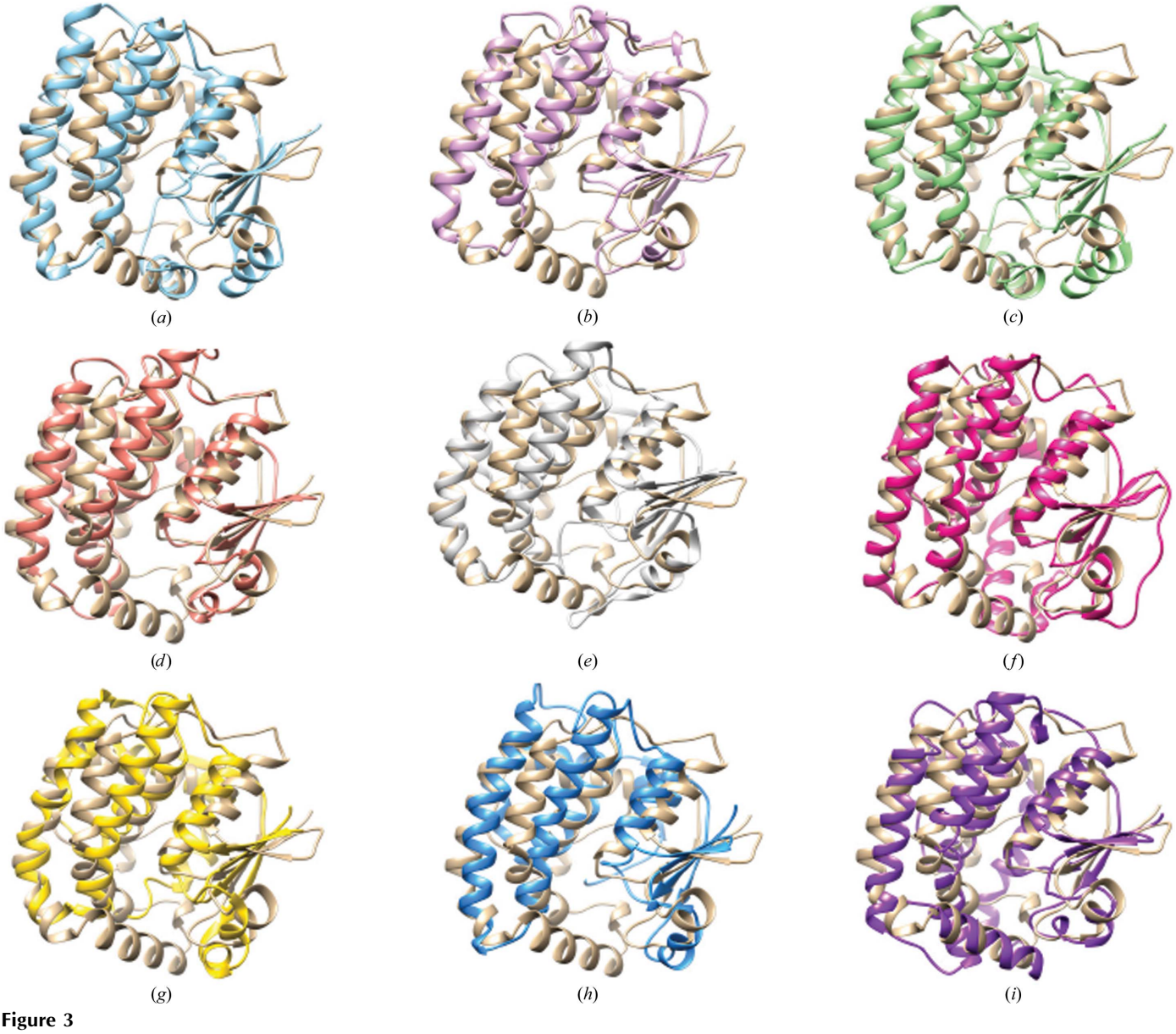

Figure 3
Comparison of the Grx2 structure with those of GSTs. Grx2 (PDB entry 4kx4; tan) was compared with representive members of the (*a*) alpha (1gse, 3.8 Å), (*b*) beta (2pmt, 3.1 Å), (*c*) delta (2wju, 3.9 Å), (*d*) phi (1gnw, 3.2 Å), (*e*) mu (1hna, 3.2 Å), (*f*) omega (1eem, 3.3 Å), (*g*) pi (1glp, 3.4 Å), (*h*) sigma (1gsq, 3.5 Å) and (*i*) theta (PDB entry 1ljr, 3.4 Å) GST classes. The PDB codes and r.m.s.d. relative to Grx2 are given in parentheses.

and Lys126 makes a water-mediated interaction with an acetate ion. However, in the Grx2 C9S/C12S structure only one interaction of Lys126 with the Tris buffer ion was observed. Therefore, the extended helix in Grx2–GSH may in part be owing to the presence of GSH and in part to the salt bridge between Lys125 and the carboxylate O atom of the glycyl residue of GSH. This conformational change may explain how GSH interacts with Lys125 in helix α5. In the Grx2–GSH structure helix α5 is more extended and its compactness is stabilized by a salt bridge formed between Lys125 and the carboxylate O atom of the glycyl residue of GSH. In contrast, in both the Grx2 C9S/C12S structure and the NMR structure (Xia *et al.*, 2001), neither of which contains a bound GSH molecule, helix α5 is more flexible by the extension of the linker.

3.3. Comparison with GST structures

Structural homology searches using the *DALI* online server (Holm *et al.*, 2006) showed that Grx2 is similar to the structures of GSTs even though they have little sequence similarity. The r.m.s.d. between Grx2 and different types of GSTs are in the range 3.0–4.0 Å (Fig. 3). The thioredoxin-like fold of the N-terminal domain of Grx2 corresponded to this region in all types of GSTs. In the C-terminal domain, the three-helix bundle (α4, α6 and α7) and helix α8 are common to Grx2 and all types of GSTs. However, theses helices are arranged in a different manner or topology in Grx2 and different GSTs. In the Grx2 structure, the C-terminus ends with a 3_{10}-helix, but in GSTs there are one or more α-helices at the C-terminus (Fig. 3). Helix α5 in Grx2 is distinguished from all types of GSTs except for human theta-class GST (PDB entry 1ljr; Rossjohn, McKinstry *et al.*, 1998). The orientation of the C-terminal α-helix of 1ljr coincides with helix α5 of Grx2, but the topology of these helices in these structures is different. In Grx2 the helix is placed between helices α4 and α6, while in 1ljr it is placed at the end of the domain.

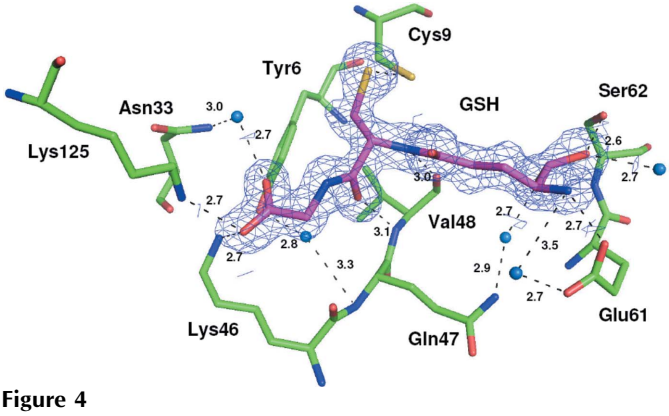

Figure 4
Structural overview of the interactions of GSH with Grx2. Bound GSH with an electron-density map ($2F_o - F_c$) contoured at the 1σ level is shown in stick representation and colored magenta (carbon), red (oxygen) and blue (nitrogen). The blue spheres represent water molecules. A potential hydrogen-bond network around the GSH molecule is indicated with dashed lines (the distances are in Å) and residues interacting with GSH are labeled.

3.4. GSH binding site (G-site)

GSH makes extensive interactions with residues from the N-terminal domain of Grx2 (Fig. 4). The O atoms of the α-carboxylate group of the GSH glutamyl residue are hydrogen bonded to the main-chain amino group and the side-chain hydroxyl group of Ser62. The N-terminal amino group of GSH makes a hydrogen bond to the side chain of Glu61. The main-chain amino and carboxyl groups of the cysteine residue make hydrogen bonds to the backbone of Val48. The carboxylate O atom of the GSH glycyl residue interacts with both Lys46 from the C-terminal domain and Lys125 from the C-terminal domain. The distance between the S atoms of the GSH cysteinyl residue and Cys9 is 2.98 Å, which is too long for a typical disulfide bond (2.05 Å). Six water molecules also interact with different regions of the GSH molecule. The distance between the S atom of Cys9 and that of Cys12 is 3.6 Å, which is also too long for a disulfide bond. However, the possibility that the synchrotron radiation has broken a disulfide bond between Cys12 and either Cys9 or GSH cannot be excluded. In the above-mentioned Grx2–GSH interactions, the two corresponding residues equivalent to Grx2 residues Cys9 and Val48 that interact with GSH are conserved in *E. coli* Grx1 (Xia *et al.*, 1992) and Grx3 (Nordstrand *et al.*, 1999) (Supplementary Fig. S4).

Structural alignment of Grx2 with members of different classes of GSTs using *STRAP* (Gille & Frömmel, 2001) shows that the GSH binding residues are similar (Supplementary Fig. S5). Of the six Grx2–GSH interactions, three interactions are structurally conserved in all GSTs. Firstly, the interaction of the carboxylate O atoms of the GSH glutamyl residue with either a serine or threonine residue (Grx2 residue Ser62) is conserved. Secondly, the N-terminal amino group of GSH interacts with a glutamine or glutamate residue in all GSTs. Thirdly, the main-chain atoms of cysteinyl residues interact with hydrophobic residues such as valine, leucine and methionine. The carboxylate O atom of the glycyl residue of GSH interacts with a lysine in several GSTs [PDB entries 1eem (Board *et al.*, 2000), 2pmt (Rossjohn, Polekhina *et al.*, 1998), 1glp (García-Sáez *et al.*, 1994), 1gsq (Ji *et al.*, 1995), 1hna (Raghunathan *et al.*, 1994) and 2wju (Tars *et al.*, 2010)] and an arginine residue in others [PDB entries 1ljr (Rossjohn, McKinstry *et al.*, 1998) and 1gse (Cameron *et al.*, 1995)]. However, this interaction is not structurally conserved. Overall, the residues in Grx2 that interact with GSH are conserved or partially conserved in GSTs. GSH binding residues Cys9, Lys46, Val48, Glu61 and Ser62 in Grx2 are only conserved in human omega-class GST.

3.5. Hydrophobic binding site (H-site)

In general, GSTs have a binding site for hydrophobic substrates (H-site) and their topologies are accessible by a wide range of substrates (Rossjohn, McKinstry *et al.*, 1998). The only substrate for Grx2 identified to date is the ArsC S–As(V) complex. The Grx2–GSH and Grx2 C9S/C12S structures have an acetate anion and a 2-amino-2-hydroxymethyl-propane-1,3-diol (Tris) cation, respectively, in their H-site.

Table 2
GST activity of Grx2 and sjGST.

	Substrate					
	GSH			CDNB		
Protein	K_m (m*M*)	k_{cat} (s^{-1})	k_{cat}/K_M (s^{-1} mM^{-1})	K_m (m*M*)	k_{cat} (s^{-1})	k_{cat}/K_M (s^{-1} mM^{-1})
Grx2	0.31	0.58	1.9	2.0	0.41	0.21
sjGST	0.28	2.6	9.3	1.1	3.4	3.1

Residues from α7 (Gln174, Pro177, Leu178, Arg180, Leu182, Asn181 and Leu184), α4 (Leu90, Asn94, Ala97, Asn98, Leu101, Leu102 and Phe105), α5 (Phe122 and Lys126) and α1 (Pro10, Tyr11, Cys12 and Lys14) define the H-site. These hydrophobic and charged residues form a narrow cleft. In the Grx2–GSH structure, the acetate ion was placed in the cleft, interacting with residue Asn98 and making van der Waals interaction with glutathione. In the Grx2 C9S/C12S structure, the Tris molecule interacts with Lys126 and Ser12.

3.6. Conformational changes upon GSH binding

Comparison of the crystal structures of the Grx2–GSH complex and Grx2 C9S/C12S indicates how binding of GSH triggers a conformational change from coil to α-helix. In the absence of GSH, the loop that connects helices α4 and α5 is extended and provides flexibility for movement of helix α5. In this conformation, the core of the structure is now easily accessible to GSH. In the GSH-bound conformation, there is a salt bridge between the carboxylate O atom of the glycyl residue of GSH and Lys125 in helix α5.

3.7. Grx2 has GST activity

The ability of Grx2 to function as a GST was examined by conjugation of GSH with the model substrate CDNB (Table 2). Purified Grx2 exhibited K_m values of 2 m*M* for CDNB and 0.31 m*M* for GSH. Grx2 was compared with an authentic GST, the *S. japonicum* GST (sjGST). The two enzymes had nearly the same affinity for GSH. The Grx2 turnover number as a function of GSH concentration was approximately 20% of that of sjGST, although it was somewhat lower for the artificial substrate CDNB. These results demonstrate that Grx2 has reasonable GST activity.

3.8. *In silico* docking analysis of the ArsC–Grx2 interaction

In *E. coli*, the ArsC arsenate reductase transforms arsenate to arsenite using GSH as the source of reducing potential (Shi *et al.*, 1999). In the catalytic cycle, glutaredoxins participate by deglutathionylation of the predicted ArsC Cys12 S–As(III)–SG complex (Martin *et al.*, 2001). Grx2 has a considerably higher affinity for ArsC than Grx1 or Grx3 and is the likely *in vivo* source of electrons for ArsC-catalyzed arsenate reduction (Shi *et al.*, 1999). It should be emphasized that to date no other physiological function has been identified for Grx2. To predict how Grx2 might interact with ArsC, the two proteins were blindly docked (rigid-body docking), with the highest ranking solution shown in Fig. 5. In this solution the catalytic residues of both proteins were found to face each other. The distance between the catalytic residues Cys12 in ArsC and Cys9 in Grx2 is 13.7 Å, and the distance between Cys12 in ArsC and the Cys residue from the tripeptide Glu-Cys-Gly, which was used to represent GSH, is 12.4 Å. When the GSH analogue molecule is rotated (in *Coot*) with respect to its long axis, its thiolate is direct towards the catalytic residue Cys12 of ArsC and the distance between them is reduced to 6.6 Å. The GSH binding residues Glu61 and Ser62 and the active-site residue Tyr11 of Grx2 are present at the interface, and these residues may assist in the predicted exchange of GSH from ArsC to Grx2. Other Grx2 residues in the C-terminal domain, including Glu170, Lys99, Asn98, Asn94 and Arg91, are also predicted to interact with ArsC. Docking of ArsC with only the N-terminal thioredoxin-like domain of Grx2 did not yield reasonable models. This may explain why Grx2 is the preferred glutaredoxin for ArsC rather the smaller Grx1 or Grx3 proteins, which lack a GST-like C-terminal domain.

4. Discussion

In *E. coli*, ArsC reduces pentavalent arsenate to trivalent arsenite with GSH as the source of reducing potential (Oden *et al.*, 1994). The reaction requires a glutaredoxin as an electron donor to regenerate the active enzyme, and in *E. coli* Grx2 is highly preferred over Grx1 or Grx3. The proposed ArsC reaction scheme includes four steps and three intermediates (Martin *et al.*, 2001). In first step, arsenate directly attacks the thiolate of the active-site residue Cys12. The

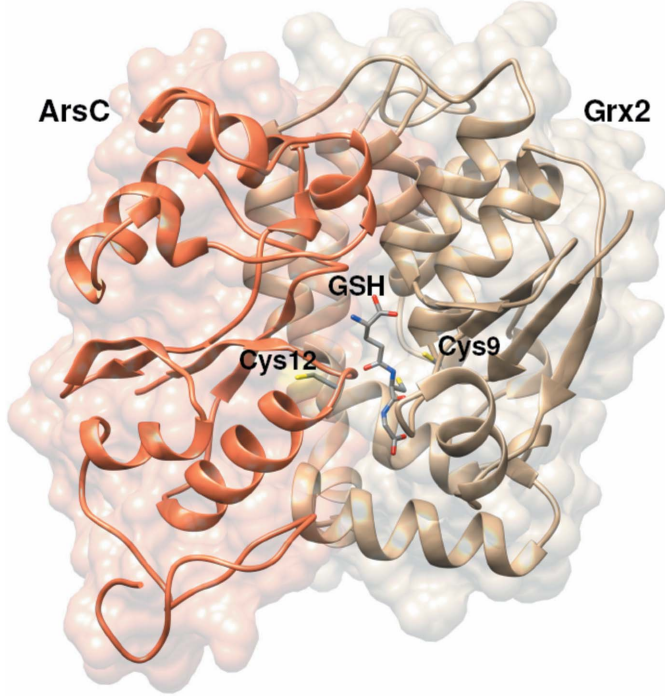

Figure 5
In silico analysis of the interaction of ArsC and Grx2 by molecular docking. Both ArsC (cyan) and Grx2 (tan) are represented by ribbon diagrams within the visible surface. Both ArsC Cys12 and Grx2 Cys9–S–SG are shown as sticks.

second step involves glutathionylation to form the active-site intermediate ArsC Cys12 S–As(V)–SG. The third step is the deglutathionylation of the complex by Grx2 and formation of the ArsC Cys12–S–As(III) intermediate, with concomitant formation of the mixed Grx2–S–SG disulfide. Interestingly, the Grx2–GSH complex only crystallized in the presence of sodium arsenate, although arsenate was not observed in the final structure. This may reflect a specific interaction with As(V), but another possibility is that arsenate serves as an electron acceptor during disulfide-bond formation. Is there direct interaction of ArsC and Grx2 during the catalytic cycle? *In silico* docking analysis of ArsC with Grx2 suggests that these two form a tight complex in which the ArsC active-site residue Cys12 and the glutathione binding residues of Grx2 face each other. A Glu-Cys-Gly tripeptide representing the glutathione moiety is located between the two proteins, and an As atom would be expected to bridge the gap.

Structurally, Grx2 is related to both glutaredoxins and GSTs. Overall, Grx2 is structurally similar to GSTs in spite of a lack of sequence similarity, and its activity with the model substrate CDNB demonstrates that Grx2 is a GST. The GSH binding residues of Grx2 are best conserved in the structure of human omega-type GST, and the orientation of the C-terminal α-helices are best matched with the structure of human theta-type GST. Thus, Grx2 does not appear to belong to any known type of GST, suggesting that it may form a new class of GST with a unique function as both a glutaredoxin and a glutathione *S*-transferase. A novel feature of Grx2 is that it is a hybrid of the small N-terminal glutaredoxin domain and the C-terminal GST domain. In *E. coli* Grx2 is the major glutaredoxin, both in terms of intracellular concentration, where it comprises two thirds of the total cytosolic glutaredoxin, and in terms of activity, where it provides 81% of the total glutaredoxin activity (Åslund *et al.*, 1994). Grx2 exhibits GST activity with about 20% of the activity of purified *S. japonicum* sjGST (Table 2). It has a relatively low catalytic efficiency (about 10% of that of sjGST), but its relatively high intracellular concentration compensates. Does this hybrid Grx/GST activity have physiological relevance? In the proposed reaction scheme for ArsC arsenate reductase activity, the second step is glutathionylation of the Cys12–As(V) intermediate and the third step is deglutathionylation of the Cys12–As(III)–SG intermediate. We propose that Grx2 serves as a glutathione *S*-transferase in the glutathionylation reaction of the second step and as a glutaredoxin in the deglutathionylation reaction of the third step, a novel mechanism for participation of the hybrid Grx/GST in arsenic detoxification.

References

Adams, P. D. *et al.* (2010). *Acta Cryst.* D**66**, 213–221.

Åslund, F., Ehn, B., Miranda-Vizuete, A., Pueyo, C. & Holmgren, A. (1994). *Proc. Natl Acad. Sci. USA*, **91**, 9813–9817.

Åslund, F., Nordstrand, K., Berndt, K. D., Nikkola, M., Bergman, T., Ponstingl, H., Jörnvall, H., Otting, G. & Holmgren, A. (1996). *J. Biol. Chem.* **271**, 6736–6745.

Board, P. G. *et al.* (2000). *J. Biol. Chem.* **275**, 24798–24806.

Cameron, A. D., Sinning, I., L'Hermite, G., Olin, B., Board, P. G., Mannervik, B. & Jones, T. A. (1995). *Structure*, **3**, 717–727.

DeLano, W. L. (2002). *PyMOL*. http://www.pymol.org.

Emsley, P., Lohkamp, B., Scott, W. G. & Cowtan, K. (2010). *Acta Cryst.* D**66**, 486–501.

Fernandes, A. P., Fladvad, M., Berndt, C., Andrésen, C., Lillig, C. H., Neubauer, P., Sunnerhagen, M., Holmgren, A. & Vlamis-Gardikas, A. (2005). *J. Biol. Chem.* **280**, 24544–24552.

Fernandes, A. P. & Holmgren, A. (2004). *Antioxid. Redox Signal.* **6**, 63–74.

García-Sáez, I., Párraga, A., Phillips, M. F., Mantle, T. J. & Coll, M. (1994). *J. Mol. Biol.* **237**, 298–314.

Gille, C. & Frömmel, C. (2001). *Bioinformatics*, **17**, 377–378.

Habig, W. H., Pabst, M. J. & Jakoby, W. B. (1974). *J. Biol. Chem.* **249**, 7130–7139.

Holm, L., Kääriäinen, S., Wilton, C. & Plewczynski, D. (2006). *Curr. Protoc. Bioinformatics*, Unit 5.5. doi:10.1002/0471250953.bi0505s14.

Holmgren, A. (1976). *Proc. Natl Acad. Sci. USA*, **73**, 2275–2279.

Humphrey, W., Dalke, A. & Schulten, K. (1996). *J. Mol. Graph.* **14**, 33–38.

Ji, X., von Rosenvinge, E. C., Johnson, W. W., Tomarev, S. I., Piatigorsky, J., Armstrong, R. N. & Gilliland, G. L. (1995). *Biochemistry*, **34**, 5317–5328.

Lundström-Ljung, J., Vlamis-Gardikas, A., Åslund, F. & Holmgren, A. (1999). *FEBS Lett.* **443**, 85–88.

Mannervik, B. & Danielson, U. H. (1988). *CRC Crit. Rev. Biochem.* **23**, 283–337.

Martin, J. L. (1995). *Structure*, **3**, 245–250.

Martin, P., DeMel, S., Shi, J., Gladysheva, T., Gatti, D. L., Rosen, B. P. & Edwards, B. F. (2001). *Structure*, **9**, 1071–1081.

Murshudov, G. N., Skubák, P., Lebedev, A. A., Pannu, N. S., Steiner, R. A., Nicholls, R. A., Winn, M. D., Long, F. & Vagin, A. A. (2011). *Acta Cryst.* D**67**, 355–367.

Navaza, J. (2001). *Acta Cryst.* D**57**, 1367–1372.

Nordstrand, K., Åslund, F., Holmgren, A., Otting, G. & Berndt, K. D. (1999). *J. Mol. Biol.* **286**, 541–552.

Oden, K. L., Gladysheva, T. B. & Rosen, B. P. (1994). *Mol. Microbiol.* **12**, 301–306.

Pettersen, E. F., Goddard, T. D., Huang, C. C., Couch, G. S., Greenblatt, D. M., Meng, E. C. & Ferrin, T. E. (2004). *J. Comput. Chem.* **25**, 1605–1612.

Phillips, J. C., Braun, R., Wang, W., Gumbart, J., Tajkhorshid, E., Villa, E., Chipot, C., Skeel, R. D., Kalé, L. & Schulten, K. (2005). *J. Comput. Chem.* **26**, 1781–1802.

Pierce, B. G., Hourai, Y. & Weng, Z. (2011). *PLoS One*, **6**, e24657.

Raghunathan, S., Chandross, R. J., Kretsinger, R. H., Allison, T. J., Penington, C. J. & Rule, G. S. (1994). *J. Mol. Biol.* **238**, 815–832.

Rossjohn, J., McKinstry, W. J., Oakley, A. J., Verger, D., Flanagan, J., Chelvanayagam, G., Tan, K.-L., Board, P. G. & Parker, M. W. (1998). *Structure*, **6**, 309–322.

Rossjohn, J., Polekhina, G., Feil, S. C., Allocati, N., Masulli, M., Di Illio, C. & Parker, M. W. (1998). *Structure*, **6**, 721–734.

Sheng, J., Ye, J. & Rosen, B. P. (2007). *Acta Cryst.* F**63**, 280–282.

Shi, J., Vlamis-Gardikas, A., Åslund, F., Holmgren, A. & Rosen, B. P. (1999). *J. Biol. Chem.* **274**, 36039–36042.

Ströher, E. & Millar, A. H. (2012). *Biochem. J.* **446**, 333–348.

Tars, K., Olin, B. & Mannervik, B. (2010). *J. Mol. Biol.* **397**, 332–340.

Vlamis-Gardikas, A., Åslund, F., Spyrou, G., Bergman, T. & Holmgren, A. (1997). *J. Biol. Chem.* **272**, 11236–11243.

Wilce, M. C. J. & Parker, M. W. (1994). *Biochim. Biophys. Acta*, **1205**, 1–18.

Xia, B., Vlamis-Gardikas, A., Holmgren, A., Wright, P. E. & Dyson, H. J. (2001). *J. Mol. Biol.* **310**, 907–918.

Xia, T.-H., Bushweller, J. H., Sodano, P., Billeter, M., Björnberg, O., Holmgren, A. & Wüthrich, K. (1992). *Protein Sci.* **1**, 310–321.